

# Machine Learning Based Channel Modeling for Vehicular Visible Light Communication

Bugra Turan, *Student Member, IEEE*, Sinem Coleri, *Senior Member, IEEE*

**Abstract**—Optical Wireless Communication (OWC) propagation channel characterization plays a key role on the design and performance analysis of Vehicular Visible Light Communication (VVLC) systems. Current OWC channel models based on deterministic and stochastic methods, fail to address mobility induced ambient light, optical turbulence and road reflection effects on channel characterization. Therefore, alternative machine learning (ML) based schemes, considering ambient light, optical turbulence, road reflection effects in addition to inter-vehicular distance and geometry, are proposed to obtain accurate VVLC channel loss and channel frequency response (CFR). This work demonstrates synthesis of ML based VVLC channel model frameworks through multi layer perceptron feed-forward neural network (MLP), radial basis function neural network (RBF-NN) and Random Forest ensemble learning algorithms. Predictor and response variables, collected through practical road measurements, are employed to train and validate proposed models for various conditions. Additionally, the importance of different predictor variables on channel loss and CFR is assessed, normalized importance of features for measured VVLC channel is introduced. We show that RBF-NN, Random Forest and MLP based models yield more accurate channel loss estimations with 3.53 dB, 3.81 dB, 3.95 dB root mean square error (RMSE), respectively, when compared to fitting curve based VVLC channel model with 7 dB RMSE. Moreover, RBF-NN and MLP models are demonstrated to predict VVLC CFR with respect to distance, ambient light and receiver inclination angle predictor variables with 3.78 dB and 3.60 dB RMSE respectively.

**Index Terms**—Vehicular visible light communication, channel modeling, machine learning based wireless communication, data driven channel modelling.

## I. INTRODUCTION

Vehicular visible light communication (VVLC) is a promising communication technology, aiming simultaneous data transmission and illumination through vehicle light emitting diode (LED) lights. VVLC is considered as a secure complementary technology to radio frequency (RF) communications due to its RF interference free nature, license free wide spectrum availability, non-frequency selective flat fading, and directional line-of-sight (LoS) channel characteristics.

Fundamentally, wireless communication channel models can be classified into two categories : deterministic and stochastic channel models. A deterministic channel model aims to predict the channel characteristics in a specific location with respect to transmitter and receiver locations, as well as the surrounding environment, exploiting computational electromagnetics with ray tracing and finite-difference time-domain (FDTD) methods. However, deterministic channel models lack

computational efficiency and heavily depend on site-specific geometry with dielectric properties of scatter materials. On the other hand, stochastic approaches are utilized to reproduce the statistical behaviors of the channel yielding non site-specific but lower accuracy models. Stochastic channel models are classified into geometry based stochastic models (GBSM) where ensemble of the scatterers are placed in different geometrical positions based on statistical distributions and non-GBSM fit measured or generated channel parameters into certain probability distributions. Stochastic approaches confront challenges with incorporating all relevant channel features. GBSM highly depend on the probabilistic distributions of physical parameters (i.e. transmitter - receiver distance, angle, scatterer locations), whereas non-GBSM stochastic channel models lack instantaneous channel spatial consistency, as all channel parameters in one channel realization are generated for a single location [1]. Considering the required effort to obtain various probabilistic distributions for different environments, stochastic channel models generally rely on certain assumptions, where channel parameters are fitted, averaged out for generalized environments and possible scenarios, lacking precision. Moreover, mathematical expressions and probability distribution fitting constraints impose additional assumptions on the stochastic models, leading limited accuracy.

Recently, machine learning (ML) methods are proposed for channel modelling to overcome site-specific, high complexity limitations of deterministic approaches and low accuracy limitations of stochastic models [2]. Moreover, highly complicated mediums such as in-body, underwater, vehicle to vehicle (V2V) [3], optical and molecular communication channels [4], inherent certain distortion effects which are challenging to be expressed analytically. Therefore, ML based channel modelling aims to develop low-complexity and accurate models for complicated channels, through direct learning of the robust patterns in the data without imposing any assumptions on the analytical expressions. Moreover, ML models distinguish over scenarios by providing physical parameters corresponding to the specific scenario as inputs.

Channel modelling with ML can be classified into supervised and unsupervised learning based with respect to the labels of training data. Supervised learning based channel modelling, aims to learn a general function between inputs and outputs yielding solution for regression problems such as path loss predictions through labeled data [5], [6]. On the other hand, unsupervised learning based channel modelling is favorable for clustering of multi path components (MPCs) with same features such as delay, angle of arrival, and angle of departure, where unlabeled large amount of data is utilized

B. Turan and S. Coleri are with the Department of Electrical and Electronics Engineering, Koc University, Sariyer, Istanbul, Turkey.  
E-mail: bturan14@ku.edu.tr, scoleri@ku.edu.tr

[7].

To date, deterministic and stochastic visible light communication (VLC) channel characterization is investigated for indoor [8]–[10], underground mine [11], [12] and outdoor [13]–[21] environments mainly through simulation based studies.

Deterministic VLC channel models are investigated through ray tracing [13]–[15], recursive methods [11], [12], [16], [22] and empirically [17], [19]–[21], [23] with site-specific measurements. Ray tracing based VLC channel modelling, yields channel impulse response (CIR) with respect to the detected power of each ray and path lengths from source to detector considering reflections. To date, ray tracing has been used to extract VLC channel delay profiles for intelligent transportation systems (ITS) applications in [13], CIR for VVLC channel under fog and rain conditions in [14], path loss model for VVLC in [15]. On the other hand, recursive methods yield power delay profile (PDP) where LoS response is computed first and multiple bounces of light through reflecting elements are computed recursively with the assumption of same reflective characteristics (i.e. Lambert surface) for all reflectors and scatterers. In the VLC recursive channel modeling literature, indoor VLC received power and time dispersion parameters are obtained through time domain simulations in [9] and frequency domain simulations in [22]. Moreover, in the recursive channel model literature, VVLC channel received power is modeled under the consideration of realistic headlight pattern and road reflection conditions in [16], underground mine VLC LoS channel path loss and shadowing parameters are extracted with respect to Mie scattering and diffraction in [11], and non-line-of-sight (NLoS) channel path loss model based on Lambertian radiation pattern is proposed in [12]. Empirical VLC channel models further investigate real world effects on VLC channel through measurements. Empirically, authors in [17] provided a path loss model for traffic light to vehicle VLC link including background solar radiation effects for a sunny day at specific location. Furthermore, [19], [20] provided VVLC channel coherence time, auto correlation function and received power with respect to vehicle movements on a 18 km pre-defined route, driven 5 times. [21] provided VVLC channel time dispersion parameters through frequency domain channel sounding for specific time of day and location. Memedi *et. al.* derived an empirical VVLC channel path loss model through stationary night measurements for unique environment, yielding received signal strength (RSS) with respect to transmitter – receiver angle and distance [23]. However, considering core dependency of VVLC channel model on channel loss due to ambient light and atmospheric effects (i.e. fading, scintillation) with mobility, ray tracing based studies lack consideration of solar radiation and optical turbulence effects on VLC link. Moreover, recursive methods rely on assumptions such as Lambertian reflection for all surfaces while empirical models represent only the small portion of usage scenarios for deterministic models.

On the other hand, stochastic channel models offer increased flexibility, reduced computational complexity, and lower accuracy when compared to deterministic approach. VLC and Optical Wireless Communication (OWC) stochastic channel models are explored in [10], [18], [24]. Considering Non-

GBSM, [10] investigated impacts of mobility on indoor VLC channel with respect to probabilistic movements for shadowing and blocking, yielding cumulative distribution function (CDF) of RSS for a range of people density. Moreover, authors in [24] proposed a statistical method to obtain CIR where Rayleigh and Gamma distributions are utilized to fit measured CIR for an indoor OWC channel. Under the consideration of GBSM, [18] proposed a 2D Non-Stationary GBSM to generate CIR for VVLC channel obtained Gaussian distributions for channel gain and root mean square (RMS) delay spread.

Considering the limited applicability of deterministic and stochastic methods on VVLC channel models due to site-specific characteristics and low accuracy, ML based channel model frameworks with the capability of learning complex features pave the way to accurately model VVLC channel propagation.

To date, ML based OWC channel modelling has not been investigated in the literature. However, ML based channel model frameworks trained through measurement data sets, on contrary to relying numerous assumptions are proposed for RF communications [3], [4], [25]–[30]. Considering millimeter-wave (mmWave) communication channels, Huang *et. al.* proposed an artificial neural network (ANN) enabled channel model framework, to obtain channel parameters including received power, RMS delay and angle spreads achieving 1.64 dB root mean square error (RMSE) for received power estimations [25]. Authors in [26] proposed convolutional neural network (CNN) based three-dimensional mmWave massive multiple input multiple output (MIMO) channels framework yielding 0.34 dB to 3.05 dB RMSE for channel path loss with transmitter and receiver location inputs under the consideration of 5 different ray tracing based data sets. For mobile channel modelling, path loss predictions through ANN is demonstrated to outperform statistical and OkumuraHata model with maximum error of 22 dB, mean error of 0 dB with 7 dB standard deviation in [27]. ANN aided hybrid signal strength prediction at 1140 MHz is depicted to provide 8 dB average improvement when compared to pure ITU-R.526-11 model in [28] whereas, an ANN based propagation model for 450, 850, 1800, 2100, and 2600 MHz yields path loss predictions with 0.235 dB absolute mean error in [29]. For vehicular communication channels, authors in [30] proposed an ANN based channel model outperforming generalized gamma, polynomial fitting and dual slope distance-break point models for path loss predictions. Ramya *et. al.* showed that non-parametric learning based Random Forest method, increased V2V channel path loss prediction accuracy with 2.2 dB mean and 1.5 dB standard deviation of absolute error when compared to log distance path loss model [3]. On the other hand, [4] proposed an ANN based molecular communications channel model to predict channel model parameters accurately, where obtaining exact analytical channel model is challenging. Thereby, ML can be regarded as an appealing approach for accurate and computationally efficient wireless communication channel modelling.

Taking into account the considerable amount of work in the VLC channel modelling literature, none of the studies to date, characterized VVLC links targeting V2V with respect to various ambient light, exhaust plume induced optical turbu-

lence, inter-vehicular distance, receiver inclination angle, lane occupancy conditions and LED frequency response through practical road measurements. Hence, this work presents ML based frameworks to extract VVLC channel signal attenuation as a function of distance, LoS - Directed Line of Sight (DLoS) conditions through receiver inclination angle, LED modulation frequency, occupied lane, optical turbulence and ambient light. VVLC channel frequency response and path loss measurements conducted via production vehicle LED lights in real road scenarios are utilized to train and validate ML based models. Proposed channel model frameworks are directly learned from measurement data sets yielding higher accuracy than slope intercept fits proposed for VLC channel. Furthermore, a comparative study between Random Forest non-parametric learning method and two types of neural networks (NNs), multilayer perceptron (MLP), radial basis function (RBF) is conducted to model VVLC channel path loss. The goal is to obtain a ML based VVLC channel propagation model framework that is not overly complex but still generalizes well and is accurate enough for practical VVLC applications. In this work we leverage the use of ML techniques towards channel path loss and channel frequency response estimation, to accurately model VVLC channel with respect to given physical conditions. In particular, we propose exploiting ML to predict VVLC link quality depending on features of ambient light, inter-vehicular distance, transmitter receiver geometry, and modulation frequency, to enable better utilization of the VVLC channel.

- We extracted the importance of predictor variables to obtain VVLC channel loss and channel frequency response (CFR) through measured VVLC propagation channels. We fit the measured channel loss data to current VLC channel models, and demonstrated that the current models do not capture channel loss deviations due to mobility and environment induced variations. This is the first work to provide a measurement based quantitative analysis of VVLC channel under various ambient lighting, optical turbulence through exhaust plume, inter-vehicular distance, and geometry with both LoS and DLoS conditions.
- We proposed MLP, RBF NN and Random Forest learning based channel model frameworks to be trained with the predictor variables of inter-vehicular distance, geometry, ambient light, optical turbulence existence, lane occupation and receiver inclination angle features yielding highly accurate channel loss and channel frequency response for the cases that proposed frameworks were not trained with. This is the first study to propose ML based VVLC channel propagation models.
- We evaluated the validity and performance of the proposed models with their sensitivity to the amount of training data. This is the first work to analyze the validity and robustness of ML based channel model frameworks for VVLC channels across a wide range of varying physical conditions.

The remainder of this paper is organized in the following way. Section II outlines the VVLC channel differences from RF vehicular communication channels and other VLC channels, highlighting the unique challenges of VVLC channel modelling. Data collection details for VVLC channel characterization and the features utilized to annotate measurement data are detailed in Section III. Existing channel path loss models and their comparison to measurement data is provided in Section IV. Section V introduced ML based channel characterization methodology, where detailed system model is can be found in Section VI. Performance evaluation and comparisons of the proposed channel model frameworks can be found in Section VII. Finally, Section VIII concludes the paper.

## II. VEHICULAR VLC CHANNEL MODELLING

### A. Vehicular VLC Channel

Vehicles are operated in varying weather, climate, illumination and road conditions. Mainly, atmospheric interaction yielding a combination of absorption and scattering plays an important role on VVLC channel characteristics. VVLC channel characterization and utilization further depends on optical turbulence, ambient light induced noise, transmitter-receiver geometry, and low pass frequency response characteristics of LEDs and optical receivers.

Optical turbulence, sourced by random temperature fluctuations on road surface and around exhaust plumes distort VVLC signals, resulting optical power fluctuations [31]. However, accurate characterization of optical turbulence and finding a mathematical expression to incorporate into VVLC channel model is challenging, due to mobility induced abrupt temperature, wind, weather changes.

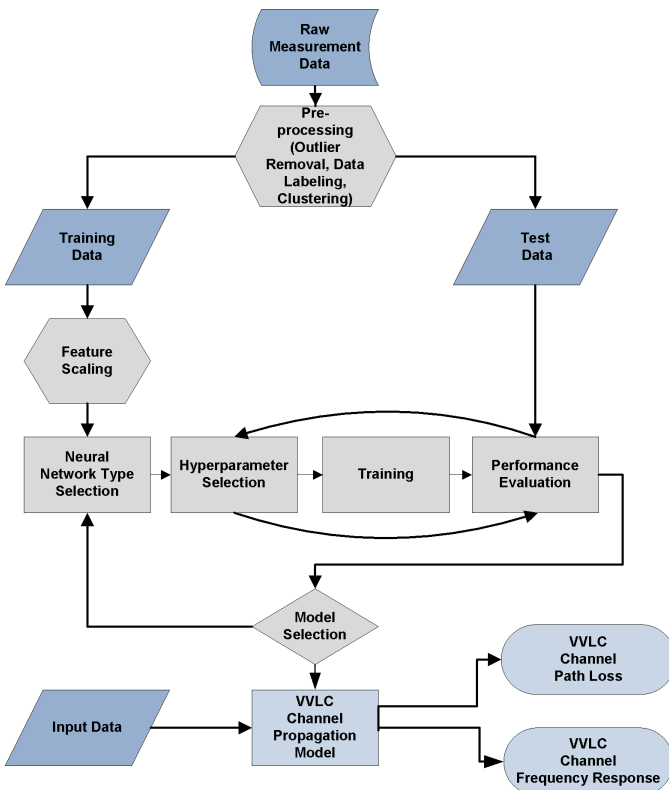


Figure 1: ML Based VVLC Channel Propagation Modelling.

The main novelties and contributions of this work are as follows.

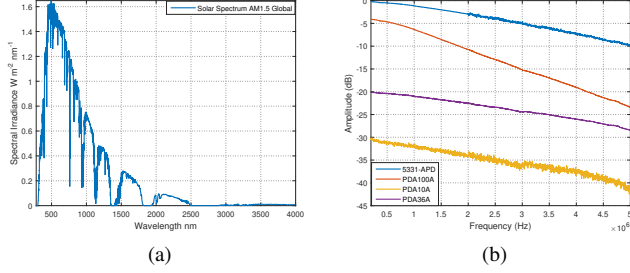


Figure 2: (a) Solar Spectrum (b) Various Optical Detectors Frequency Response for Vehicle LED Headlight

More photons from sun light reaches to optical detector during day time. Thus, the number of photons to reach the optical receiver from VVLC transmitter decreases. Moreover, photons absorbed from ambient lights and solar radiation excite electrons and cause them to generate current in the form receiver shot noise and thermal noise. Sunlight contamination dominates the noise and determines the number of photons captured by the receiver for daylight conditions. As solar spectrum (See Fig.2a) is stronger in the visible light region, optical sun interference filters, that attenuate communication signals are not favorable for practical VVLC systems. Therefore, with the increase in ambient light, less photons from VVLC signals reach to the receiver, and dynamic range of the VVLC receiver decreases due to increased receiver noise, leading more channel loss.

Fig.2b depicts the difference between various optical receivers (Hamamatsu C-5331 APD, Thorlabs PDA100A, Thorlabs PDA36A, Thorlabs PDA10A) with respect to same optical signal swept from 100 kHz to 5 MHz at fixed distance and ambient light conditions. It is clear that, due to receiver aperture, spectral responsivity and inherent gain stage of the receivers, VVLC channel loss and frequency response depends on the receiver selection. Hence, VVLC channel loss, incorporating receiver noise in addition to propagation loss due to atmospheric attenuation and fading should be considered for VVLC channels.

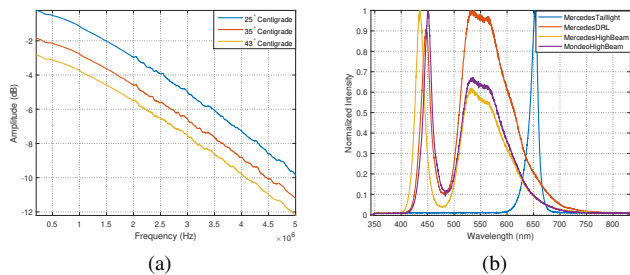


Figure 3: (a) Production vehicle LED headlight frequency response degrades with the increasing temperature (b) Spectrum of various vehicle LEDs depicts the difference between LEDs of same purpose (i.e. headlight)

Vehicle LED light half intensity beam angle (HIBA), regulation [32] driven minimum illumination field of view (FoV), with the utilization of beam shaping optics such as lenses, reflectors and mirrors determine LoS and DLoS characteristics

of VVLC channel. Compared to indoor and underwater VLC channels, diffuse components sourced from nearby scatters is weak for VVLC channels. Hence, VVLC channels are mainly explored for their LoS characteristics. Low pass frequency response of both LEDs and optical receivers impose additional limitations on the VVLC received optical signal power, as high frequency modulated signals are transmitted and received with lower optical power. LED temperature dependent characteristics [33] (See Fig.3a) and varying spectral properties of each automotive LED (See Fig.3b) further determines VVLC link performance and channel loss.

Multipath fading poses limitation on RF based vehicular communication system performance due to different transmitter and receiver geometries, mobility, nearby scatter objects, and dynamic propagation conditions. However, VVLC, utilizing non-coherent vehicle LED lights, and receiver apertures in the order of millions of wavelengths, is immune to multipath fading with no small fading [34]. Even though, multipath fading is not a major concern for VVLC, multipath dispersion, sourced from the transmitted signals outreach to the receiver via different paths and times cause symbols spreads, yielding intersymbol interference (ISI). Road surface with different reflection properties and nearby scatters such as guard rails and vehicles can be considered as main source of multipath dispersion for VVLC. However, considering the low amplitude of MPCs when compared to strong LoS signals, multipath dispersion has subtle ISI effects on practical VVLC inter-vehicular distances (i.e. 10 m to 100 m).

On the other hand, high Doppler spread in vehicular environments for RF based vehicular schemes, induces short channel coherence time, requiring accurate channel estimation for reliable communications. However for VVLC, considering 650nm wavelength taillight LED, at a vehicle speed of 250km/h, yields 210MHz Doppler frequency or 0.00015nm wavelength shift from its nominal value. Since the optical receiver detects only the intensity of the optical wave, the generated photo current will deviate from the expected level based only on the spectral sensitivity (A/W) of the receiver. Even though this results with electrical signal to noise ratio (SNR) variation at the receiver side, as the wavelength shift due to Doppler spread is subtle, Doppler spread can be regarded negligible for VVLC channels.

VVLC channels exhibit unique characteristics among vehicle to everything (V2X) communication channels, in terms of their ambient light and atmospheric dependencies where analytical characterization and generalizations lead challenges.

Fig. 4 shows the relation between LED modulation frequency, ambient light and channel DC gain at the inter-vehicular distance of 6 m, where channel DC gain is observed decrease with increasing ambient light and modulation frequency. Fig.9 represents the correlation between channel loss and ambient light for each measurement distance of LoS VVLC channel. Unlike RF V2X channel models, characterization of Doppler Spread and multipath fading is not targeted for VVLC channel characterizations. Moreover, ensuring directional long distance optical communications, channel loss characterization poses more importance than time dispersion parameter extraction, which is not the case for indoor VLC

channels.

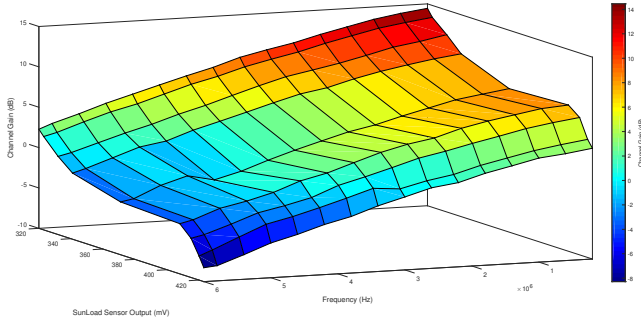


Figure 4: Channel Gain at 6m under Varying Ambient Light

### III. CHANNEL MEASUREMENTS AND MEASURED DATA STATISTICS

#### A. Channel Loss Measurements

Two different measurement campaigns are executed to capture VVLC channel properties. Static frequency domain VVLC channel sounding is conducted to obtain channel frequency response with respect to varying inter-vehicular distance and ambient light conditions. On the other hand dynamic RSS based measurement campaigns targeted characterization of VVLC channel loss for various ambient light, receiver angle, optical turbulence region and lane occupation conditions. Moreover, dynamic RSS based channel loss measurements aim to investigate the effects of both LoS and DLoS propagation where receiver is inclined towards road surface to capture optical signals both from LoS and road surface reflections. Two different data sets of dataset 1 (DS1) for CFR and dataset 2 (DS2) for channel loss characterizations. Data sets DS1 and DS2 are formed through field measurements of 29631 and 61488 samples respectively.

1) *Frequency Domain Measurements*: Frequency domain VVLC channel measurements are handled by a closed loop vector network analyzer (VNA) based approach to accurately characterize VVLC channel path loss dependence on modulation frequency. At the transmitter, Port 1 of Rohde & Schwarz ZNB20B or Anritsu 2026-C VNA is connected to a 47dB amplifier which consists of two cascaded low noise amplifiers (LNAs) considering their 1dB compression point. The output of the amplifier is connected to bias-tee where the DC-bias voltage is selected at the linear working region of the LED. The resulting signal is fed to a MY2017 Ford Mondeo LED headlight. At the receiver, Hamamatsu S3884 – C5331 avalanche photo detector (APD) is utilized to capture the optical signal. The output of the utilized photo detector is connected to a 25dB Mini Circuits ZFL500 LNA to increase SNR of the captured signal. Amplifier output is fed to Port 2 of the VNA using three Huber-Suhner Sucoflex 404 shielded microwave cables.

The measurements are taken under the same calibration with same cables and connectors. The VNA is operated at  $-20\text{dBm}$  output power mode. For all measurements,  $N_f=4001$  samples are recorded with 5 averaging for each sweep to reduce random

noise. intermediate frequency (IF) bandwidth is selected as 500 Hz, enabling  $-70\text{ dB}$  noise floor level.

$S_{21}$  parameter measurements at 1411 different points are taken for LED modulation frequencies between 2 kHz - 10 MHz from 2m (i.e. bumper to bumper traffic) to 20m (i.e. platoon distances) distances at various background light levels including outdoor sunny day, night time with ambient lights on and off, sunrise, sunset, and cloudy weather. However, considering limited modulation bandwidth of vehicle LED light under interest, measurement points between 2 kHz - 2 MHz with 100 kHz step sizes are employed for channel frequency response and channel loss characterization forming DS1.

Path loss measurement campaign yielded, frequency dependent path loss ( $-S_{21}$ ) of VVLC channel with respect to inter-vehicular distance and sun load sensor outputs. DS1 is composed of 29631 samples of 21 variables, where 1411 measurement points are considered with 19 channel loss magnitude variables for LED modulation frequencies between 2 kHz- 2 MHz (100 kHz intervals), with distance and sun load sensor predictor variables.

2) *RSS Measurements*: For dynamic VVLC channel RSS measurements, Rohde Schwarz FSV-3 vector signal analyzer (VSA) with Hamamatsu S3884 – C5331 APD is employed at the receiver vehicle where 1 MHz sinusoidal tone generated from arbitrary waveform generator (AWG) is fed to a vehicle LED day time running light (DRL) through LED current driver at the transmitter vehicle. Measurements up to 114 m inter-vehicular distances are captured through remote control of VSA with LabView software where global positioning system (GPS) locations are fed from GPS disciplined oscillator of NI USRP 2932 software defined radio, accelerometer and production vehicle sun load sensor voltage values are recorded with NI MyRIO real time embedded controller. Considering limited accuracy of GPS receiver, Velodyne VLP-16 Lidar is utilized for distance measurement and range validations. Our VVLC channel sounding setup is detailed in [21].

As VVLC channel RSS also depends on angular variations sourced through road surface (i.e. bumps), accelerometer values are recorded to observe road surface and driving style dependent VVLC signal RSS fluctuations where extreme variations are considered to be outliers. Dynamic measurements are composed of four different scenarios including LoS same lane leader follower, DLoS same lane leader follower, LoS next lane leader follower, DLoS next lane leader follower, where receiver inclination angle is  $30^\circ$  for DLoS conditions to better capture road surface reflections and decrease sun light interference, similar to production vehicle's rear view camera orientations. Either transmitter or receiver vehicle is located at a fixed location while the other is moved with a maximum velocity of 10 km/s up to 114 m distance during dynamic scenario measurements. For dynamic scenarios 7686 RSS values are captured. Measurement setup specifications are summarized in Table I. DS2 is composed of 61488 measurement samples, where distance, ambient light, occupied lane and receiver angle are predictor variables, and channel loss is the response variable, x, y, z axis acceleration measurements are validation variables to detect outlier samples.

Table I: Measurement Setup Front End Specifications

Parameter	Value
<b>Transmitter</b>	
Headlight 3-dB Bandwidth	2 MHz
DC Bias Voltage	24 V
Driver Block Input Signal Amplitude	63 mV <sub>pp</sub>
Driver Block Total Gain	47 dB
Driver Block Output Signal Amplitude	14.1 V <sub>pp</sub>
LED Input Signal Amplitude	5.6 V <sub>pp</sub>
LED Optical Transmitted Power	-6.72 dBm
Transmitter Height	0.7 cm
<b>Receiver</b>	
Avalanche Photodiode Module	Hamamatsu C5331-03
APD Active Area	1 mm
APD 3 dB Frequency Bandwidth	4kHz to 100 MHz
APD Spectral Response Range	400 to 1000 nm
APD Peak Sensitivity Wavelength	800 nm
Amplifier	Mini-Circuits ZFL-1000LN+
Amplifier Gain	20 dB
Amplifier Frequency Range	0.1 to 1000 MHz
Receiver Height	0.7 m

Table II: Measurement Data Statistics

Measurement Data	Path Loss (dB)						Max Distance (m)	Number of Path Loss / RSS Measurement Points
	200 kHz		1 MHz		2 MHz			
	$\mu_{200k}$	$\sigma_{200k}$	$\mu_{1M}$	$\sigma_{1M}$	$\mu_{2M}$	$\sigma_{2M}$		
DS1- Night (SL <300 mV)	7.82	13.07	8.98	13.27	11.09	13.66	20	998
DS1- Day (SL >300 mV)	20.25	13.84	21.59	14.11	23.83	14.21	20	413
DS2 (Day-Night)	-	-	50.81	17.89	-	-	114	7686

The features we annotate RSS and CFR measurements are,

- 1) **Intervehicular Distance:** (a number in meters 50 cm - 114 m) the distance between the transmitter and receiver vehicles, calculated from GPS locations, laser distance finder and LiDAR point clouds.
- 2) **Ambient Light:** (a number in millivolt) voltage values increases with the solar radiation and ambient light, where the value changes between 33 (complete darkness) to 475 (sun shine, clear sky).
- 3) **Receiver Inclination Angle:** (a number in degrees) the optical receiver elevation angle, varied between 0 °for LoS and 30 °for DLoS.
- 4) **Occupied Lane:** The vehicles are either located in the same lane denoted as 1, or nearby lane denoted with 0.
- 5) **Optical Turbulence:** Optical turbulence sourced by vehicle exhaust is observed to be substantial when receiver vehicle equipped with optical detector at the rear of the vehicle moves in reverse direction, due to exhaust plumes scattering, optical turbulence existence is labeled as 1 whereas the non-existence is denoted with 0.
- 6) **Variance Region:** Nearby distance amplitude measurements are observed to have high variance, where k-means clustering unsupervised ML algorithm detailed in Section VI-C is utilized to label high variance region with 1, and the rest as 0.
- 7) **VNA Model** Two different VNAs are utilized for CFR measurements, labeled as 1 or 0.  $S_{21}$  parameter amplitude differences are observed due to varying LED driving capability and non-accurate calibrations of VNAs, regarding low impedance LED loads.

#### IV. EXISTING CHANNEL PATH LOSS MODELS AND COMPARISON TO MEASUREMENT DATA

The path loss between a VVLC transmitter and receiver originates from free-space attenuation, scattering, angular orientation and ambient light induced receiver noise.

To date, VVLC channel path loss is modeled with Lambertian model, linear fitting, exponential and two term exponential fitting. Lambertian model is modified with respect to vehicle optics at Piecewise Lambertian model [35] and channel DC gain is expressed as,

$$H(0) = \frac{(n+1)A}{2\pi D^\gamma} \cos^n \phi \cos(\theta) \quad (1)$$

where  $n$  is the Lambertian model order given as  $n = -\frac{\ln 2}{\ln \cos(\phi_{1/2})}$ ,  $\phi_{1/2}$  is the LED half power angle,  $\gamma$  is the path loss exponent,  $A$  is the receiver aperture size,  $\phi$  is the incidence angle,  $\theta$  is the irradiance angle, and  $D$  is the inter-vehicular distance. For piece wise Lambertian model,  $n$  and  $\gamma$  are extracted through linear least square method.

Linear VVLC channel path loss model proposed in [14] is given by  $P_r = P_t(\alpha d + \beta)$ , where  $P_r$  is received power,  $P_t$  is transmitted power,  $d$  is the inter-vehicular distance,  $\alpha$  and  $\beta$  are weather dependent coefficients.

On the other hand, exponential model proposed in [15] is given as,

$$P_r = P_t A d^{-2B} \exp(-cd) \quad (2)$$

where  $d$  is intervehicular distance,  $c$  is the weather dependent extinction coefficient (i.e.  $1.5 \times 10^{-5}$  for clear weather),  $A$  is geometrical loss, and  $B$  is the decaying factor.

Two term exponential model is also proposed for VVLC path loss characterization [21]. The channel DC gain of two term exponential model has the following form,

$$H(0) = a_1 e^{a_2 D} + a_3 e^{a_4 D} \quad (3)$$

where  $a_1$ ,  $a_2$ ,  $a_3$  and  $a_4$  are fitting coefficients,  $D$  is the inter-vehicular distance.

Fig. 5 depicts normalized path loss of DS1 and path loss of DS2 as a function of inter-vehicular distance along with the best fit of two term exponential model for DS1 and all considered model fits for DS2 under all ambient light conditions.

Fig. 6 (a) shows the CDF of experimental power variation of DS1 in decibels normalized between  $-1dB$  to  $1dB$ . On the other hand Fig. 6 (b) depicts the path loss power variations of DS2 measurements for LoS and same lane scenarios up to 20 m, similar conditions to DS1. The power variation denotes the difference between measured path loss and best fit through two term exponential fit in Fig. 5. CDF of power variations are compared to the frequently used normal random variable, where they are observed to deviate. Comparing power variation CDF of two different data sets, it can be concluded that statistical generalization of VVLC channels with respect to distance lacks accuracy due to different vehicle LED light optics, background illumination, geometric orientation and optical turbulence.

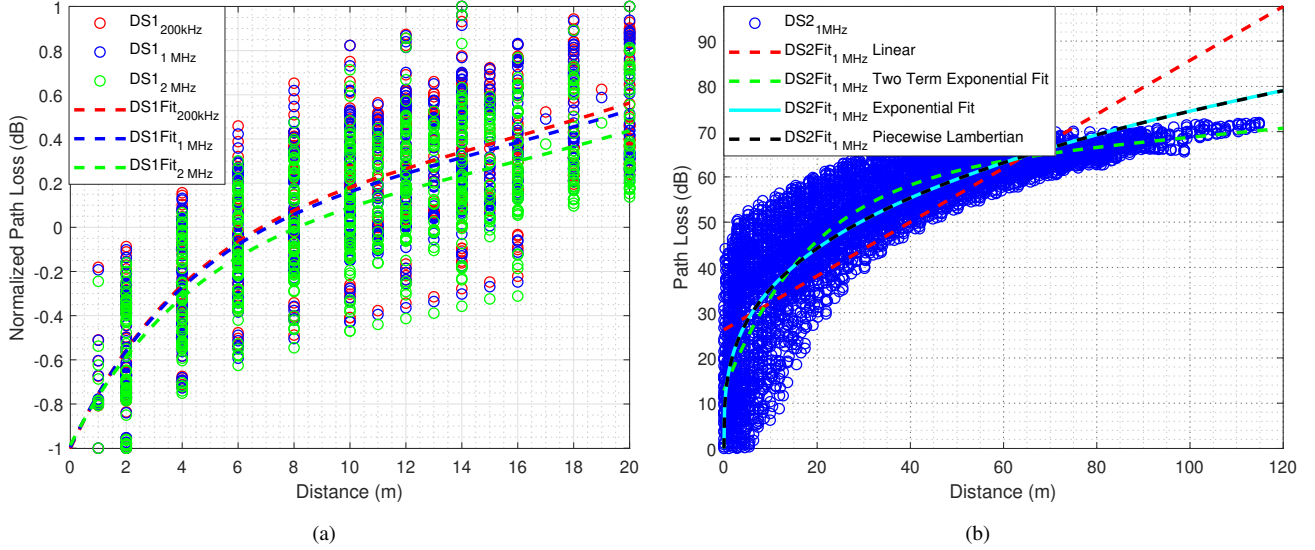


Figure 5: (a) Dependence of Dataset 1 path loss on the distance and modulation frequency with two term exponential fit (b) Dependence of Dataset 2 path loss on the distance with linear, two term exponential, exponential and piecewise Lambertian fit

Table III: Fitted Coefficients for Existing Channel Models

Method	Parameter	DS1 <sub>200kHz</sub>	DS1 <sub>1MHz</sub>	DS1 <sub>2MHz</sub>	DS2 <sub>1MHz</sub>
Piecewise Lambertian	n	45.1	49.04	20.8	5.883
	$\gamma$	1.158	1.119	0.7838	0.3243
Exponential Fitting	A	1.148	1.151	1.182	0.5971
	B	0.8586	0.8373	0.7536	0.1619
Linear Fitting	$\alpha$	-0.06007	-0.0585	-0.05492	0.5954
	$\beta$	0.5061	0.5092	0.5393	26.21
Two Term Exponential	a	-0.1549	-0.1419	-0.09861	60.34
	b	0.0656	0.06706	0.07597	0.0013
	c	1.156	1.138	1.085	-47.57
	d	-0.2282	-0.2276	-0.2191	-0.05405

Both static and dynamic scenario data sets, DS1, DS2, with varying inter-vehicular distances are evaluated as benchmark for piecewise Lambertian, linear, exponential and two-term exponential models. Normalized channel path loss  $[-1dB - 1dB]$  of DS1 is considered in order to provide fair comparison due to different VNA usage through measurements.

Table III shows the coefficients for existing VVLC channel models extracted through least squares fit. Path loss exponent and Lambertian model order are observed to vary with respect to modulation frequency for Piecewise Lambertian model. Decaying factor (B) of exponential model is obtained close to 0.87 of [15] for 200 kHz and 1 MHz modulation frequencies of DS1, where it decreases with the increasing modulation frequency.

Table IV depicts RMSE and norm of residuals (NoR) for DS1, RMSE and Coefficient of Determination (R-Squared) ( $R^2$ ) for DS2 fittings of considered models. RMSE represents the standard deviation of residuals while  $R^2$  determines how close the data is to the fitted regression line. Considering RMSE, NoR and  $R^2$  as goodness of fit metrics, two term exponential fitting outperforms the other models for both data sets and all modulation frequencies.

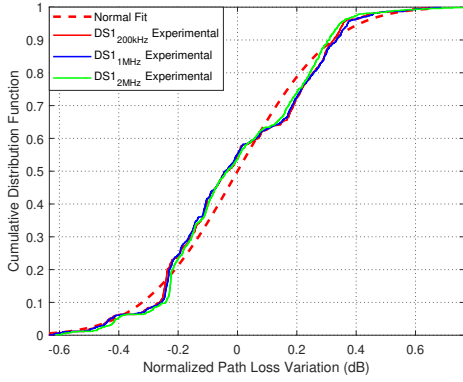
Fig. 7 (a) depicts distance dependent path loss for all dynamic scenarios of DS2, it can be observed that most of the path loss variations occur below 20m distance, where the optical beam is relatively narrow. Moreover, Fig 7 (b) reveals

that road surface reflections increase DLoS RSS for closer distances in same lane, whereas for nearby lane scenarios, both LoS and DLoS scenarios exhibit similar characteristics, indicating substantially weaker RSS than LoS scenarios. Fig 7 (c) shows path loss variations of DS2 with all scenarios for two term exponential fit with the comparison of unit variance Normal distribution. All scenarios of DS2 is observed to have less power deviation than Normal distribution with unit variance. Moreover, nearby lane path loss power variations are slightly lower than same lane path loss power variations for both LoS and DLoS scenarios indicating a better fit for two term exponential. DS2 fitting results indicate that, for night conditions, path loss variations below 20m and same lane scenarios is higher when compared to weaker illumination region of nearby lane and distances over 20m. Therefore, it can be concluded that fitting based generalizations are not enough to obtain accurate VVLC channel path loss.

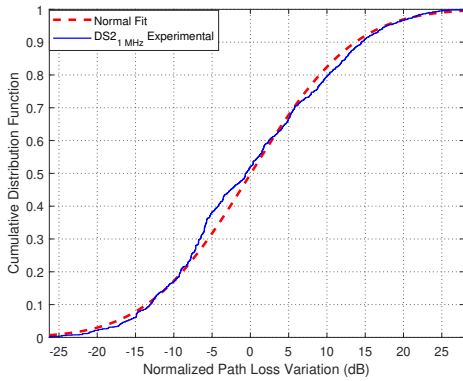
Existing channel models lack incorporating all features of ambient light, LED frequency dependent characteristics, optical turbulence effects and reflections (i.e. road surface) with respect to receiver orientation angle effects on VVLC channel. Thus, they provide limited generalization ability to accurately characterize VVLC channel path loss. Therefore, VVLC channel models generated with the consideration of ambient noise, LED frequency dependent propagation, inter-vehicular distances and transmitter - receiver geometry (i.e. LoS, DLoS) with respect to atmospheric interactions (i.e. turbulence, scintillation) are expected to yield more accurate channel characterization.

## V. METHODS AND DESIGN

Continuous movement of vehicles leads varying inter-vehicular distances, orientation angles and different ambient light levels. VVLC channel path loss and channel frequency response modeling can be classified as a regression problem,



(a)



(b)

Figure 6: (a) CDF of the Dataset 1 Fit Normalized Path Loss Variations (b) CDF of the Dataset 2 Fit Path Loss Variations for LoS up to 20 m

Table IV: Measured Channel Path Loss Goodness of Fit Metrics

Method	DS1 <sub>200kHz</sub>		DS1 <sub>1MHz</sub>		DS1 <sub>2MHz</sub>		DS2 <sub>1MHz</sub>	
	RMSE	NoK	RMSE	NoR	RMSE	NoR	RMSE	R-Square
Piecewise Lambertian	0.4283	11.87	0.4175	11.58	0.3841	10.65	7.457	0.8539
Exponential Fitting	0.3933	10.90	0.3804	10.54	0.3334	9.24	7.459	0.8538
Linear Fitting	0.2671	7.40	0.2677	7.42	0.2536	7.03	10.220	0.7254
Two Term Exponential	0.2512	6.95	0.2522	6.98	0.2394	6.63	7.002	0.8712

yielding relationship between path loss, ambient light, LED modulation frequency, transmitter-receiver distance and geometries with respect to the VVLC front ends under consideration. Obtaining an analytical expression, denoting channel path loss and channel frequency response with respect to transmitter-receiver vehicle geometries, ambient light, and optical turbulence considerations is not convenient. Hence, modeling the physical parameter relationships by NNs and Random Forest through machine learning is utilized. Therefore, channel loss data collected from different VVLC scenarios are used to train ML models, yielding a scenario based VVLC channel path loss and CFR framework. We describe the proposed ML based channel model frameworks in Section V-A, and Section V-B.

## A. Neural Networks Based Channel Model Framework

Neuron is the basic component and processing unit of NNs. Neurons produce an output vector of NNs through multiplication of input vector  $X = (x_1, x_2, \dots, x_n)$  and its weight vectors  $W = (w_1, w_2, \dots, w_n)$ , where differentiable activation functions  $f(\cdot)$  between layers and bias  $\theta$  to shift activation function are additionally employed can be generalized in the following form;

$$y = f_{oj} \left[ \sum_{j=1}^M w_{oj} \left( f_{ji} \left[ \sum_{i=1}^N w_{ji} x_i \right] + \theta_j \right) + \theta_{out} \right] \quad (4)$$

where,  $f_{oj}$ ,  $w_{oj}$  and  $f_{ji}$ ,  $w_{ji}$  are activation functions and weights from neuron to output, input to neuron respectively. Minimization of the output error according to target optimization criteria (i.e. mean square error, mean absolute percentage error) is the objective of neuron models.

Two NN architectures, MLP and RBF NNs are proposed to generalize VVLC channel path loss and channel frequency response.

1) *MLP*: MLP networks are feed-forward NNs comprise of multiple hidden layers, involving three stages. At the first stage, input training pattern is feed-forwarded using activation functions, then associated error and weights are backpropagated through learning function. Outputs are compared with target values where the weights are readjusted to minimize the error at each iteration. Activation function is selected to be monotonically non decreasing and differentiable. For regression problems, sigmoid function in the hidden layers and linear function in the output layers are utilized. MLPs, unlike simple perceptron, are capable of classifying linearly inseparable, multivariate patterns and can solve complicated problems.

2) *RBF-NN*: Radial basis function neural networks (RBF-NNs) are three-layer feed-forward networks where the input is transformed by radially symmetric basis functions at the hidden radial basis layer. RBF-NNs consist of an input layer, a hidden radial basis layer with a non-linear RBF activation function and a linear output layer.

The number of nodes in the hidden layer depends on the complexity of the problem. However, RBF-NNs generally require more neurons than standard MLP networks. This is because sigmoid neurons can have outputs over a large region of the input space, while radial basis neurons only respond to relatively small regions of the input space. RBF-NNs perform better when many training vectors are available. Designing RBF-NN takes less time than training a MLP network.

The nonlinear activation function for RBF-NN can be gaussian function, multi quadratic function, inverse multi quadratic or cauchy function. However, [36] stated that the activation function selection is not crucial for performance of the RBF-NN. Gaussian activation functions, defined by mean and standard deviation is the most common choice for RBF-NN.

In RBF NN, the connections between the input and the hidden layers are not weighted. The inputs therefore reach the hidden layer node unchanged, and then the output of

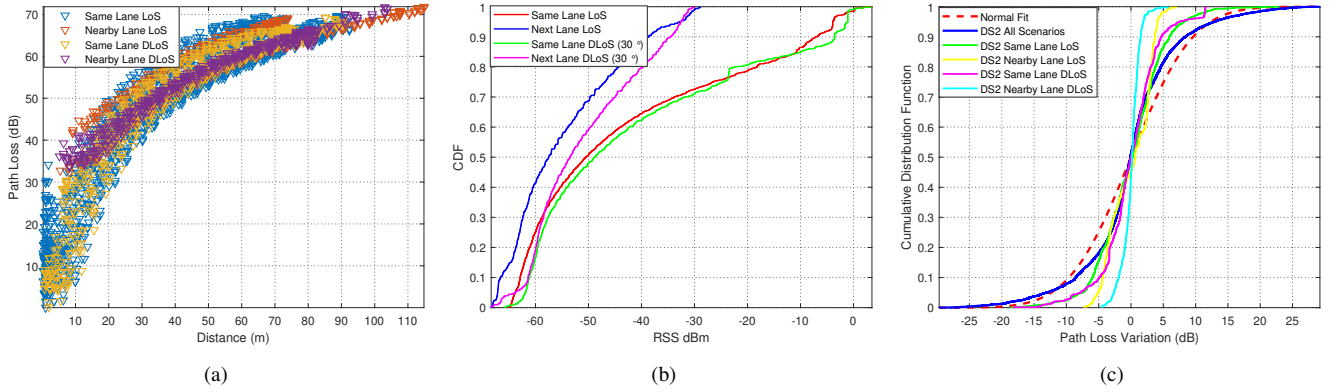


Figure 7: (a) Dataset 2 Distance Dependent Path Loss for All 4 Dynamic Scenarios (b) Dataset 2 CDF of RSS Values (c) Dataset 2 Two Term Exponential Fit Path Loss Variations CDF

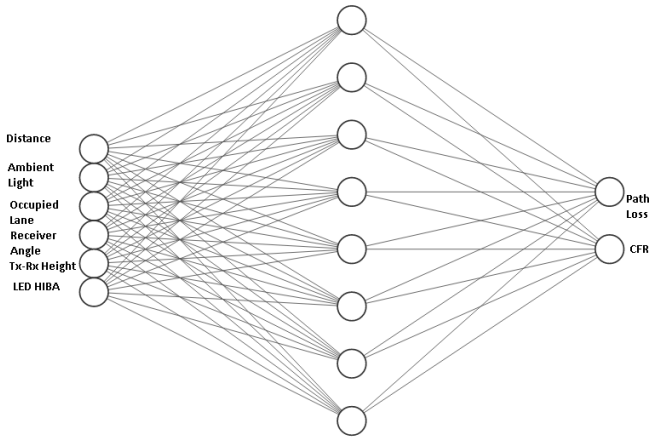


Figure 8: ANN

the hidden neuron is presented with the following activation function,

$$G_m(x) = e^{-\frac{(x-V_m)^2}{2\sigma_m^2}} \quad m = 1, 2, \dots, j \quad (5)$$

where  $X = (x_1, x_2, \dots, x_n)$  is the input data,  $V_m$  is the center of the  $m^{\text{th}}$  neuron of the hidden layer having same dimension with  $X$ ,  $\sigma_m$  is the spread of the  $m^{\text{th}}$  Gaussian, and  $G_m(x)$  is the output of the  $m^{\text{th}}$  Gaussian function,  $m$  denotes the total number of hidden layer nodes. Non-linear mapping of input layer  $X \rightarrow G_m(x)$ , whereas output layer linear mapping,  $G_m(x) \rightarrow y_k$ , forms a linear combination of hidden layer functions with weighted sums as follows;

$$y_k = \sum_{i=1}^m w_{ik} G_m(x) \quad k = 1, 2, \dots, n \quad (6)$$

where,  $y_k$  is the output of RBF-NN,  $w_{ik}$  are the weights of linear mapping,  $n$  is the number of output layer nodes.

For the input signals closer to the centre range of the Gauss kernel, the hidden layer nodes will produce larger output. Therefore, the radial basis function network is a local approaching network and it has a superiority of fast learning speed. Spread of RBF-NN defines the selectivity of

the network, as small spread implies very selective, and many neurons are needed to obtain smooth function fit. On the other hand large spread implies less selective network output, yielding smoother function approximations.

RBF-NN tend to have good interpolation properties, but not as good extrapolation properties as MLPs. Using a given number of neurons, MLP performs better for extrapolation purposes. On the other hand, RBF-NN are robust to adversarial noise, due to their non-linear nature.

### B. Random Forest Learning Based Channel Model

Ensemble learning, utilizing multiple individual decision trees to solve classification and regression problems, provide superior generalization performance due to its insensitive nature to variable scaling and inclusion of irrelevant variables [37]. Random Forest is one of the prominent ensemble learning algorithms, combining estimates from multiple decision trees with random selection of features for training to yield true output through bootstrap aggregation [38]. Randomization and averaging estimates from multiple decision trees further provide robustness to noisy measurements. The maximum tree depth and the size of the ensemble determines the accuracy of the algorithm. Random Forest algorithm sort the importance of features, enabling feature dimension reduction to avoid overfitting with lower complexity models.

## VI. SYSTEM MODEL AND PROBLEM FORMULATION

Two different model frameworks are considered yielding VVLC channel frequency response and channel path loss predictions utilizing DS1 and DS2 respectively.

### A. Channel Frequency Response Prediction Models

With the assumption of constant electrical transmit power at swept LED modulation frequencies, CFR prediction of VVLC channel is posed as a regression problem where intra-vehicular distance, ambient light and receiver angle are inputs as  $x_i : \{d_i, sl_i, \theta_i\}$ . The relationship between input  $x_i \in \mathbb{R}^3$  and CFR  $y_i \in \mathbb{R}^{19}$   $y_i : \{PL_i^{200kHz}, \dots, PL_i^{2MHz}\}$  is given by  $f_{CFR} : X \rightarrow Y$ , where the objective is to estimate  $f_{CFR}(x)$  using training dataset from DS1, minimizing the

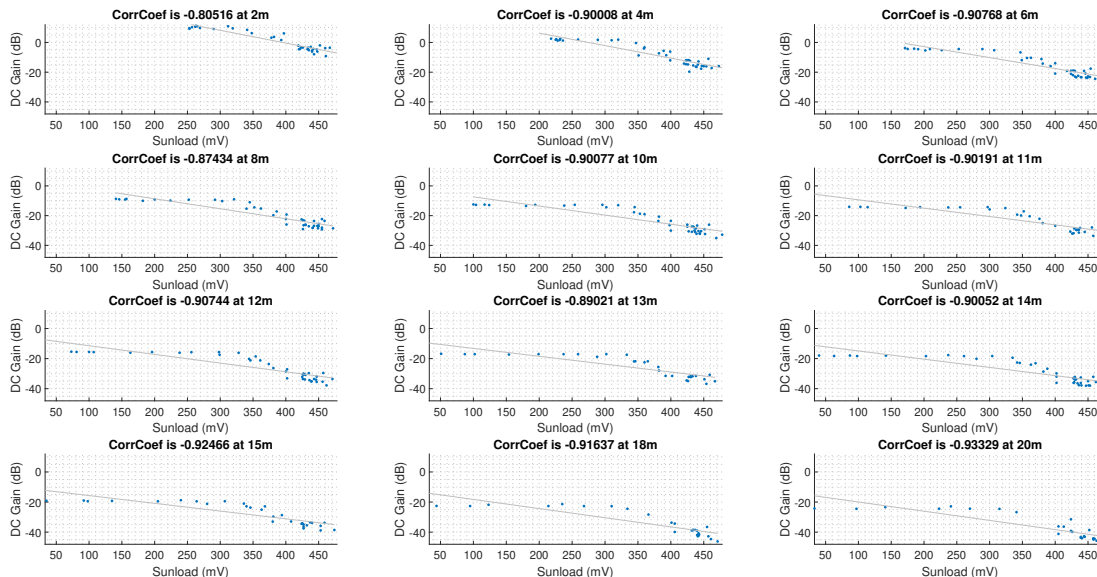


Figure 9: DS1 Ambient Light and Channel Gain Correlation at Various Distances

CFR estimation error for new input data that models are not trained with. Performance of the models are evaluated with the comparison of target values and model output  $\hat{Y}$  to input test samples through RMSE.

### B. Channel Path Loss Prediction Models

Intra-vehicular distance, LED modulation frequency, ambient light levels, occupied lane, optical turbulence level and receiver elevation angle are inputs of the proposed models, whereas model output yields channel path loss. The VVLC channel path loss predictions can be considered as function approximation where the goal is to approximate an unknown mapping  $f : X \rightarrow Y$  from a set of input parameters  $X : \{d_l, o_l, sl_l, lane_l, \theta_l\}$  to another set of channel path losses  $Y : \{PL_l\}$ , where  $d_l$  denotes inter-vehicular distance,  $o_l$  represents optical turbulence regime either low or high,  $sl_l$  contains sun load sensor voltage values indicating ambient light,  $lane_l$  is the occupied lane of receiver vehicle,  $\theta_l$  is the receiver orientation angle denoting LoS or DLoS conditions and  $PL_l$  is the path loss of VVLC channel,  $d_l, o_l, sl_l, lane_l, \theta_l$  and  $PL_l$  variables are extracted from measurement data set as input-output vector pairs to train neural network and random forest during training phase. During the testing phase, the trained network is fed an input vector of  $X : \{d_l, o_l, sl_l, lane_l, \theta_l\}$  to obtain the estimated output  $\hat{Y}$ . Performance of trained models are evaluated by comparing the estimate  $\hat{Y}$  to the actual output  $Y$  across the test data set using RMSE.

For path loss models 90%, 80%, 60%, 30% and 10% of DS2 samples are utilized for training while the rest portions (10%, 20%, 40%, 70%, 90%) are used as test set for performance evaluations.

### C. Data Preprocessing

Input values of the proposed models vary in different ranges as they are different physical units. Therefore, input parameters are normalized and mapped to values between -1 to 1. Inverse conversion is executed at the output to obtain predicted values. Outlier samples captured through measurement errors are excluded from all data sets. For path loss prediction models, high variance region is observed for closer inter-vehicular distances due to the narrower beam divergence angle. Thus, k-means clustering is utilized to further label the data as high variance region and low variance region.

1) *K-means Clustering*: K-means clustering iteratively partitions  $n$  observations into  $k$  non-overlapping clusters where each observation belongs to the cluster with the nearest mean. Expected maximization approach of k-means clustering assigns data points to a cluster where the sum of the squared distance between the data points and the mean of all the data points that belong to that cluster (centroid) is at the minimum.

K-means clustering is conducted to define low variance and high variance regions with respect to inter-vehicular distances for channel path loss prediction models. As the initial choice of centroids can affect the output clusters, the algorithm is executed 10 times with different initializations to obtain two fair cluster partitions of DS2. 3297 samples of 7686 samples is found to be in high variance region with maximum distance of 38 m whereas 4389 samples are considered in low variance regions as depicted in Fig.10. High variance and low variance region labels are added to the training data to increase regression accuracy.

2) *Predictor Importance Estimation*: Feature selection is key for both to obtain accurate results and avoid over fitting. Permutation feature importance estimation method from Random Forest is utilized to measure predictor importance [38]. For predictor importance estimation increase in the

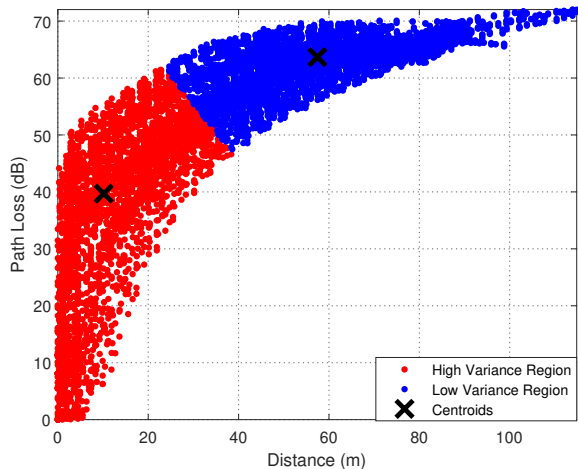


Figure 10: Low Variance and High Variance Regions of DS2 from K-means clustering algorithm

Table V: Normalized Importance of Input Features

Feature	Importance (PL)	Importance (CFR)
Distance	0.7884	0.4161
Optical Turbulence	0.0579	-
Ambient Light	0.0361	0.2804
Amplitude Variance Region	0.0883	-
Occupied Lane	0.0218	-
Receiver Inclination Angle	0.0075	0.0661
VNA Model	-	0.2375

models prediction error after permuting the feature changes is calculated.

Table V denotes the normalized predictor importance values of both data sets. Distance and amplitude variance region selection appeared to be more important features than the others for VVLC path loss. On the other hand, distance and ambient light are observed to be most important features for VVLC CFR. Moreover, VNA model feature selection is perceived to have a considerable effect on the predictor performance for CFR estimations, as VNA drives the LED through frequency swept electrical voltage signals and accurate calibrations can not be executed for low impedance LEDs on contrary to  $50\Omega$  load. Receiver angle inclination is concluded to be the least important feature for both data sets, hence, reflections from road surface can be considered to be negligible for DLoS when compared to LoS transmissions.

#### D. Hyperparameter Selection

ML model parameters, that can be selected before training process are known as hyperparameters. Grid search, random search and Bayesian optimization methods are commonly utilized for hyperparameter optimization. Hyperparameter optimization plays an important role for ML models to obtain accurate prediction results in reduced training time, while ensuring simultaneous convergence, hence avoiding over fitting.

In this work, grid search is employed to find the optimal combination of hyperparameters through search of all possible points in the given range. For MLP the following parameter intervals are considered for both CFR and path loss models

: number of neurons for 2 hidden layers between 1 to 50 and the number of maximum validation failures between 3 to 10, minimum performance gradient between  $1e-3$  to  $1e-8$  with  $1e-5$  intervals. Considering RBF-NN, selection of spread is important to obtain smoother function. Therefore, spread values are evaluated between 0.2 to 10 for both CFR and path loss estimation models. For path loss predictions with Random Forest, the number of decision trees between 150 and 300 and the maximum tree depths between 16 and 1024 are evaluated.

The optimum hyperparameters yielding best predictions are obtained as follows. For CFR prediction MLP model, 30 neurons at first hidden layer, 20 neurons at second hidden layer, whereas for 20 neurons at first hidden layer and 10 neurons at second hidden layer for CFR. Maximum validation failure of 5, minimum performance gradient of  $1e-6$  are set for both MLP networks. RBF-NN spread factor for path loss is 0.2 and 0.7 for CFR. For Random Forest, the depth of trees and the number of decision trees are finally chosen as 253 and 710, respectively for path loss predictor.

#### E. Model Implementation

We developed the proposed models using MATLAB software running on Dell T5610 workstation. The workstation is equipped with NVIDIA Quadro K2000 graphics card and 12 CPU cores, enabling parallel training on GPU and CPU multi-cores.

1) *MLP Framework for VVLC Channel Path Loss Predictions*: Data sets of MLP networks are splitted as 60% training, 20% testing and 20% validation, then the input features were scaled between  $-1$  to  $1$ . Five fold cross validation scheme is employed to determine best model for MLP.

Our network is multi-layer perceptron (MLP) type feed forward architecture. It is based on a supervised training using scaled conjugate gradient back propagation. We use hyperbolic tangent sigmoid function (Tansig) in the hidden layers and linear function (Purline) in the output layer.

MLP networks for both CFR and path loss predictions are modeled with a perceptron of three layers, two hidden layers and one output layer. The number of neurons per layer is varied to improve performance.

2) *RBF Framework for VVLC Channel Path Loss Predictions*: The RBF framework created for VVLC channel path loss predictions has the Gaussian function as activation function in its hidden layer, and linear function in its output layer. Training of the hidden layer involves the determination of the radial basis functions by specifying appropriate  $\sigma_m$  values of (5). This parameter depend only on the input data and are independent of the outputs, yielding unsupervised learning. On the other hand, output layer is trained by a supervised learning method, where the synaptic weights are updated in proportion to the difference between the network and target output. The input data is scaled between  $-1$  and  $1$ , where 70% of data sets is used for training and 30 % of the all samples are used for testing RBF-NNs.

The spread of the Gaussian for CFR estimator RBF-NN, and path loss estimator RBF-NN, is defined as 0.2 and 0.7 respectively. The training parameter goal for both networks is set to  $1e-1$ .

Table VI: MLP Based Path Loss Estimation Framework Parameters and Prediction Performance

Training Dataset (DS2)	Number of Neurons (Layer 1 -2 )	MAE (dB)	RMSE (dB)	R-Correlation Coefficient
10 %	35-20	2.7735	4.8249	0.9642
30 %	33-15	2.2874	3.9881	0.9742
60 %	31-10	2.1856	3.9502	0.9755
80 %	39-29	2.2676	4.0885	0.9746
90 %	37-20	2.2702	4.2637	0.9700

Table VII: RBF-NN Based Path Loss Framework Parameters and Prediction Performance

Training Dataset (DS2)	Number of Neurons	MAE (dB)	RMSE (dB)	R-Correlation Coefficient
10 %	289	1.8938	3.6063	0.9794
30 %	289	1.8682	3.5037	0.9807
60 %	551	1.8854	3.5305	0.9799
80 %	551	1.8606	3.5426	0.9799
90 %	551	2.2041	4.2858	0.9722

3) *Random Forest*: For Random Forest algorithm, decision tree depth denotes the number of splits made on the independent variables. The number of decision trees that their outputs are averaged over gives the size of the ensemble. Too deep trees with small ensemble size lead to detailed models with overfitting, whereas too shallow trees might yield overly simplified models that can not fit data accurately. Generally, increasing the ensemble size makes the model more robust. However, the improvement decreases after certain number of added decision trees, where the cost in computation time for learning should be considered. Random forest used 60% data for training and the rest is used for validation.

Random Forest algorithm for path loss predictions is designed with the following parameters, number of decision trees of 253, maximum number of splits of 710. Mean square error (MSE) is used as the performance criteria through 10 fold cross validations.

## VII. PERFORMANCE EVALUATION

We evaluated the performance of MLP, RBF-NN and Random Forest methods for VVLC channel path loss predictions, whereas MLP and RBF-NN models are considered for CFR estimations. RMSE and mean absolute error (MAE) metrics used to evaluate model performances are given as,

$$MAE = \frac{1}{n} \sum_{i=1}^n |T_i - O_i|$$

$$RMSE = \sqrt{\frac{1}{n} \sum_{i=1}^n (T_i - O_i)^2}$$
(7)

where,  $T_i$  is the target value of  $i$  th test sample,  $O_i$  is the model output value of the  $i$  th sample from test set,  $n$  is the total number of test set samples.

For path loss prediction models, various portions of measurement samples are randomly selected to train the network, while the rest is utilized to test the networks. Table VI depicts the performance of MLP path loss models with respect to trained data, whereas Table VII depicts the RBF-NN path loss model performance results. Both networks with various training sample sizes are observed to yield better prediction performance when compared to fitting based VVLC models. Moreover, the performance of MLP based path loss prediction model decreases with the increasing number of training

samples, indicating overfitting. Therefore, 60% of samples are considered to train both MLP and RBF-NN networks, while the rest 40% is utilized to test the network for optimum performance results. RBF-NN outperforms MLP 0.42 dB RMSE and 0.3 dB MAE for path loss predictions, considering same training and test samples for both networks. RBF-NN requires more neurons than MLP for similar prediction performance, whereas the training time of RBF-NN is substantially lower than the training time of MLP (i.e. 20 mins for RBF-NN, 13 hours for MLP)

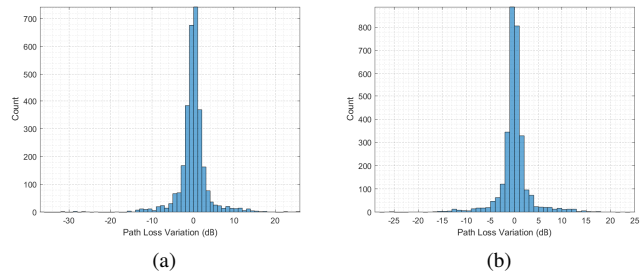


Figure 11: (a) Prediction Error Distribution of MLP Based Path Loss Model (b) Prediction Error Distribution of RBF-NN Based Path Loss Model

Table VIII: Best Path Loss Models with Optimal Hyperparameters

Algorithm	Optimal Hyperparameters	RMSE (dB)	MAE (dB)
Random Forest	Number of Estimators 253 , Maximum Depth 710	3.8107	2.4541
MLP	35-10 2 layer network, tansig activation function	3.9502	2.1856
RBF-NN	Spread Factor 0.4, NN Size 551	3.5305	1.8854

Table VIII shows the selected optimal hyperparameters along with MAE and RMSE values for each method. RBF-NN outperforms both methods, whereas Random Forest yields lower RMSE but higher MAE when compared to MLP.

Table IX depicts the performance results of MLP and RBF-NN to model CFR with selected hyperparameters. RBF-NN is observed to outperform MLP by 0.18 dB RMSE whereas MLP MAE is 0.97 dB is less than RBF-NN for CFR estimations. Therefore, CFR of a VVLC channel can be predicted with similar performance using both models with respect to ambient light, inter-vehicular distance and receiver inclination angle.

Table IX: Best CFR Models with Optimal Hyperparameters

Algorithm	Optimal Hyperparameters	RMSE (dB)	MAE (dB)
MLP	27-15 2 layer network, tansig activation function	3.7801	2.6173
RBF-NN	Spread Factor 0.2 , NN Size 55	3.6043	3.5821

MLP model for CFR predictions is observed to perform similar with reduced training data set. However, RBF-NN prediction performance degrades 0.6 dB when the training data

Table X: CFR Estimation Model Performance with Different Training Data Size

Training Data Size	Model	MAE (dB)	RMSE (dB)
30%	RBF-NN	4.1884	4.2120
70%	RBF-NN	3.5821	3.6043
30%	MLP (28-35)	2.6428	3.8027
70%	MLP (27-15)	2.6173	3.7801

size reduces from 70 % of all samples to 30 % as depicted in Table X.

### VIII. CONCLUSION

This work introduces a novel approach than traditional methods in modeling the VVLC channel loss and CFR on a practical road environment, based on ML techniques. The validation results based on experimental measurements demonstrate the efficiency of the proposed frameworks to predict or generate VVLC channel path loss with respect to relevant input parameters.

Revealing the importance of the features affecting VVLC channel performance through ensemble learning, accurate channel loss and CFR predictions can be obtained. Moreover, data acquisition for channel modelling can be executed in a systematic manner, as more concentration will be given to relatively important features. However, the importance of the features can be experimental setup dependent. Increased variance in the captured data of the feature increases its importance. For example, with wide FoV optical receiver angular orientation may be less important when compared to narrower FoV receiver. Therefore, experimental setup plays an important role for the feature importance selection and generalization ability of the ML model.

For VVLC channels, ML techniques are demonstrated to yield better generalization than fitting based models, even for the reduced amount of training data. Therefore, the main drawback of big data acquisition to train ML models is not the case for VVLC channel modelling through ML methods. Prediction accuracy obtained through the proposed ML methods can be further increased through refinement of the models with the evaluation of various algorithms and hyper parameter optimization.

Proposed ML models built and validated through real world measurements, enable new scenario based data set generation. As they are not constrained with probabilistic distributions, analytical expressions, and assumptions, parameters extracted from generated data sets and ML based channel models will be closer to field measurements.

### REFERENCES

- [1] L. Raschkowski, P. Kyösti, K. Kusume, and T. Jämsä, "Metis channel models," *ICT-317669-METIS/D1. 4*, 2015.
- [2] S. M. Aldossari and K.-C. Chen, "Machine learning for wireless communication channel modeling: An overview," *Wireless Personal Communications*, vol. 106, no. 1, pp. 41–70, 2019.
- [3] P. M. Ramya, M. Boban, C. Zhou, and S. Stańczak, "Using learning methods for v2v path loss prediction," in *2019 IEEE Wireless Communications and Networking Conference (WCNC)*. IEEE, 2019, pp. 1–6.
- [4] C. Lee, H. B. Yilmaz, C.-B. Chae, N. Farsad, and A. Goldsmith, "Machine learning based channel modeling for molecular mimo communications," in *2017 IEEE 18th International Workshop on Signal Processing Advances in Wireless Communications (SPAWC)*. IEEE, 2017, pp. 1–5.
- [5] Y. Zhang, J. Wen, G. Yang, Z. He, and J. Wang, "Path loss prediction based on machine learning: Principle, method, and data expansion," *Applied Sciences*, vol. 9, no. 9, p. 1908, 2019.
- [6] J. Wen, Y. Zhang, G. Yang, Z. He, and W. Zhang, "Path loss prediction based on machine learning methods for aircraft cabin environments," *IEEE Access*, vol. 7, pp. 159 251–159 261, 2019.
- [7] R. He, B. Ai, A. F. Molisch, G. L. Stuber, Q. Li, Z. Zhong, and J. Yu, "Clustering enabled wireless channel modeling using big data algorithms," *IEEE Communications Magazine*, vol. 56, no. 5, pp. 177–183, 2018.
- [8] A. Al-Kinani, C.-X. Wang, H. Haas, and Y. Yang, "Characterization and modeling of visible light communication channels," in *2016 IEEE 83rd Vehicular Technology Conference (VTC Spring)*. IEEE, 2016, pp. 1–5.
- [9] K. Lee, H. Park, and J. R. Barry, "Indoor channel characteristics for visible light communications," *IEEE communications letters*, vol. 15, no. 2, pp. 217–219, 2011.
- [10] P. Chvojka, S. Zvanovec, P. A. Haigh, and Z. Ghassemlooy, "Channel characteristics of visible light communications within dynamic indoor environment," *Journal of Lightwave Technology*, vol. 33, no. 9, pp. 1719–1725, 2015.
- [11] J. Wang, A. Al-Kinani, W. Zhang, C.-X. Wang, and L. Zhou, "A general channel model for visible light communications in underground mines," *China Communications*, vol. 15, no. 9, pp. 95–105, 2018.
- [12] J. Wang, A. Al-Kinani, J. Sun, W. Zhang, and C.-X. Wang, "A path loss channel model for visible light communications in underground mines," in *2017 IEEE/CIC International Conference on Communications in China (ICCC)*. IEEE, 2017, pp. 1–5.
- [13] S. Lee, J. K. Kwon, S.-Y. Jung, and Y.-H. Kwon, "Evaluation of visible light communication channel delay profiles for automotive applications," *EURASIP journal on Wireless Communications and Networking*, vol. 2012, no. 1, p. 370, 2012.
- [14] M. Elamassie, M. Karbalayghareh, F. Miramirkhani, R. C. Kizilirmak, and M. Uysal, "Effect of fog and rain on the performance of vehicular visible light communications," in *2018 IEEE 87th Vehicular Technology Conference (VTC Spring)*. IEEE, 2018, pp. 1–6.
- [15] H. B. Eldeeb, F. Miramirkhani, and M. Uysal, "A path loss model for vehicle-to-vehicle visible light communications," in *2019 15th International Conference on Telecommunications (ConTEL)*. IEEE, 2019, pp. 1–5.
- [16] P. Luo, Z. Ghassemlooy, H. Le Minh, E. Bentley, A. Burton, and X. Tang, "Performance analysis of a car-to-car visible light communication system," *Applied Optics*, vol. 54, no. 7, pp. 1696–1706, 2015.
- [17] K. Cui, G. Chen, Z. Xu, and R. D. Roberts, "Traffic light to vehicle visible light communication channel characterization," *Applied optics*, vol. 51, no. 27, pp. 6594–6605, 2012.
- [18] A. Al-Kinani, J. Sun, C.-X. Wang, W. Zhang, X. Ge, and H. Haas, "A 2-d non-stationary gbsm for vehicular visible light communication channels," *IEEE Transactions on Wireless Communications*, vol. 17, no. 12, pp. 7981–7992, 2018.
- [19] A.-L. Chen, H.-P. Wu, Y.-L. Wei, and H.-M. Tsai, "Time variation in vehicle-to-vehicle visible light communication channels," in *2016 IEEE Vehicular Networking Conference (VNC)*. IEEE, 2016, pp. 1–8.
- [20] L. Cheng, W. Viriyasitavat, M. Boban, and H.-M. Tsai, "Comparison of radio frequency and visible light propagation channels for vehicular communications," *IEEE Access*, vol. 6, pp. 2634–2644, 2017.
- [21] B. Turan, G. Gurbilek, A. Uyrus, and S. C. Ergen, "Vehicular vlc frequency domain channel sounding and characterization," in *2018 IEEE Vehicular Networking Conference (VNC)*. IEEE, 2018, pp. 1–8.
- [22] H. Schulze, "Frequency-domain simulation of the indoor wireless optical communication channel," *IEEE Transactions on Communications*, vol. 64, no. 6, pp. 2551–2562, 2016.
- [23] A. Memedi, H.-M. Tsai, and F. Dressler, "Impact of realistic light radiation pattern on vehicular visible light communication," in *GLOBECOM 2017-2017 IEEE Global Communications Conference*. IEEE, 2017, pp. 1–6.
- [24] R. Perez-Jimenez, J. Berges, and M. Betancor, "Statistical model for the impulse response on infrared indoor diffuse channels," *Electronics Letters*, vol. 33, no. 15, pp. 1298–1300, 1997.
- [25] J. Huang, C.-X. Wang, L. Bai, J. Sun, Y. Yang, J. Li, O. Tirkkonen, and M. Zhou, "A big data enabled channel model for 5g wireless communication systems," *IEEE Transactions on Big Data*, 2018.
- [26] L. Bai, C.-X. Wang, J. Huang, Q. Xu, Y. Yang, G. Goussetis, J. Sun, and W. Zhang, "Predicting wireless mmwave massive mimo channel characteristics using machine learning algorithms," *Wireless Communications and Mobile Computing*, vol. 2018, 2018.
- [27] E. Ostlin, H.-J. Zepernick, and H. Suzuki, "Macrocell path-loss prediction using artificial neural networks," *IEEE Transactions on Vehicular Technology*, vol. 59, no. 6, pp. 2735–2747, 2010.
- [28] G. P. Ferreira, L. J. Matos, and J. M. Silva, "Improvement of outdoor signal strength prediction in uhf band by artificial neural network," *IEEE Transactions on Antennas and Propagation*, vol. 64, no. 12, pp. 5404–5410, 2016.

- [29] M. Ayadi, A. B. Zineb, and S. Tabbane, "A uhf path loss model using learning machine for heterogeneous networks," *IEEE Transactions on Antennas and Propagation*, vol. 65, no. 7, pp. 3675–3683, 2017.
- [30] T. Zhang, S. Liu, W. Xiang, L. Xu, K. Qin, and X. Yan, "A real-time channel prediction model based on neural networks for dedicated short-range communications," *Sensors*, vol. 19, no. 16, p. 3541, 2019.
- [31] Z. Li, T. Lang, L. Liao, and G. Chen, "Effects of vehicle exhaust to vlc link: measurement and analysis," in *Laser Communication and Propagation through the Atmosphere and Oceans IV*, vol. 9614. International Society for Optics and Photonics, 2015, p. 96140Q.
- [32] U. E. R. No, "112, uniform provisions concerning the approval of motor vehicle headlamps emitting an asymmetrical passing beam or a driving beam or both and equipped with filament lamps," 2004.
- [33] A. M. Colaco, C. P. Kurian, S. G. Kini, S. Colaco, and C. Johny, "Thermal characterization of multicolor led luminaire," *Microelectronics Reliability*, vol. 78, pp. 379–388, 2017.
- [34] A. Al-Kinani, C.-X. Wang, L. Zhou, and W. Zhang, "Optical wireless communication channel measurements and models," *IEEE Communications Surveys & Tutorials*, vol. 20, no. 3, pp. 1939–1962, 2018.
- [35] W. Viriyasitavat, S.-H. Yu, and H.-M. Tsai, "Short paper: Channel model for visible light communications using off-the-shelf scooter taillight," in *2013 IEEE Vehicular Networking Conference*. IEEE, 2013, pp. 170–173.
- [36] S. Chen, C. F. Cowan, and P. M. Grant, "Orthogonal least squares learning algorithm for radial basis function networks," *IEEE Transactions on neural networks*, vol. 2, no. 2, pp. 302–309, 1991.
- [37] J. Friedman, T. Hastie, and R. Tibshirani, *The elements of statistical learning*. Springer series in statistics New York, 2001, vol. 1, no. 10.
- [38] L. Breiman, "Random forests," *Machine learning*, vol. 45, no. 1, pp. 5–32, 2001.